Ecotoxicology and Environmental Safety 185 (2019) 109691

Contents lists available at ScienceDirect

Ecotoxicology and Environmental Safety

journal homepage: www.elsevier.com/locate/ecoenv

Enantioselective mechanism of toxic effects of triticonazole against *Chlorella pyrenoidosa*

Rui Liu[a], Yue Deng[a,b], Wenjun Zhang[a,b], Luyao Zhang[a,b], Zikang Wang[a], Bingyan Li[c], Jinling Diao[a], Zhiqiang Zhou[a,b,*]

[a] Department of Applied Chemistry, China Agricultural University, Yuanmingyuan West Road 2, Beijing, 100193, China
[b] Beijing Advanced Innovation Center for Food Nutrition and Human Health, Yuanmingyuan West Road 2, Beijing, 100193, China
[c] College of Agronomy, Shanxi Agricultural University, Mingxian South Road 1, Shanxi, 030800, China

ARTICLE INFO

Keywords:
Ecotoxicity
Enantioselective mechanism
Triticonazole
Chlorella pyrenoidosa

ABSTRACT

The rational use and the environmental safety of chiral pesticides have attracted significant research interest. Here, enantioselective toxic effects and the selective toxic mechanism of triticonazole (TRZ) against the aquatic microalgae *Chlorella pyrenoidosa* were studied. The 96h-EC_{50} values of rac-, (R)-(−)-, and (S)-(+)-TRZ were 1.939, 0.853, and 22.002 mg/L, respectively. At a concentration of 1 mg/L, the contents of photosynthetic pigments of *C. pyrenoidosa* exposed to (R)-(−)-TRZ were lower than if exposed to S-(+)-form and racemate. Transmission electron microscopic images showed that the R-(−)-form compromised the integrity of cells and disrupted the chloroplast structure. R-(−)-TRZ stimulated vast reactive oxygen species (ROS) and significantly increased superoxide dismutase (SOD) and catalase (CAT) activities, as well as malondialdehyde (MDA) content. For lipid accumulation experiments, nicotinamide adenine dinucleotide (NADH) and triacylglycerol (TAG) accumulations in algal cells treated with R-(−)-TRZ were 171.50% and 280.76%, respectively, compared with the control group. This far exceeded levels of algal cells treated with S-(+)- and rac-TRZ. Based on these data, R-(−)-TRZ was concluded to selectively affect the photosynthetic system, antioxidant system, and lipid synthesis of algal cells, thus causing enantioselective toxic effects of TRZ against *C. pyrenoidosa*, which indicating that the use of racemate may cause unpredictable environmental harm. Therefore, to reduce the hidden dangers of chiral pesticides for the ecological environment, the environmental risk of TRZ should be evaluated at the stereoselective level.

1. Introduction

In recent decades, the consumption of pesticides has increased across the world; consequently, humans and other animals are exposed to these pesticides. However, although chiral pesticides have been reported to be stereoselective, knowledge about the risks for human health and the environment is limited (de Albuquerque et al., 2018). About 30% of the active ingredients of pesticides sold on the global market are chiral pesticides that consist of two or more enantiomers (Ye et al., 2015). In fact, due to the different biological properties, toxicities, and metabolic behaviors of enantiomers in the environment, the biological activities of chiral pesticides are only known for one or a few enantiomers in specific cases (Kurihara et al., 1999). For example, the fungicidal activity of the amide-type fungicides benalaxyl and metalaxyl is mainly caused by the R-enantiomer, while the S-enantiomer is almost inactive (Pérez-Fernández et al., 2011); the fungitoxicities of the four stereoisomers of paclobutrazol (a triazole fungicide) also differ strongly (Burden et al., 1987). Thus, it is important to explore the enantioselective behavior of these compounds in the environment to better understand safety concerns of chiral pesticides for the environment and health. Triazole fungicides form a class of systemic fungicides that contain a 1,2,4-triazole moiety and are widely used to control fungal diseases on fruits, vegetables, legumes, and cereal crops (Kahle et al., 2008). Triazole fungicides have been reported to have plant growth regulating properties. In addition to inhibiting the biosynthesis of gibberellin, triazole compounds affect the photosynthesis rate, enzymatic activity, lipid peroxidation, and yield components of carrots and herbaceous *Madagascar vinca*. Consequently, they protect plants from abiotic stresses such as drought, high temperatures, and air pollutants (Davis et al., 1988; Fletcher, 1988).

Triticonazole (TRZ) (Fig. 1) is a triazole fungicide that was developed by Bayer. The TRZ molecule contains one asymmetric center and

* Corresponding author. Department of Applied Chemistry, China Agricultural University, Yuanmingyuan west road 2, Beijing, 100193, China.
E-mail address: zqzhou@cau.edu.cn (Z. Zhou).

https://doi.org/10.1016/j.ecoenv.2019.109691
Received 25 June 2019; Received in revised form 14 September 2019; Accepted 17 September 2019
Available online 26 September 2019
0147-6513/

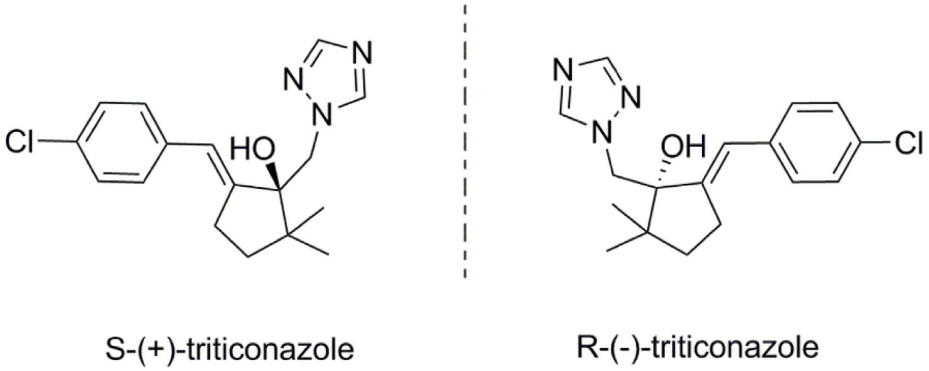

Fig. 1. Structure of the two enantiomers of triticonazole.

consists of the two enantiomers (S)-(+)-TRZ and (R)-(−)-TRZ. TRZ inhibits the steroid demethylation of plant pathogens and interferes with the biosynthesis of ergosterol, and is thus widely used for the treatment of foliage and seeds (Quérou et al., 1998).

At present, most triazole chiral pesticides are still sold and used in the form of racemates. However, although the enantiomers have the same physicochemical properties, they differ in absorption, transportation, and degradation processes due to various environmental effects; this results in different environmental behavior characteristics (Hu et al., 2010; Starr et al., 2014; Ye et al., 2010). The presence of inactive ingredients or ingredients with low activity not only increases the volume of used pesticides but also negatively impacts non-target organisms, which has resulted in many hidden dangers to human health and the ecological environment. For example, the results of Qian et al. indicated exerted R-(−)-imazethapyr had stronger toxicity on the growth of rice than S-(+)-imazethapyr (Qian et al., 2009a). Moreover, the effect of R-(−)-imazethapyr on the root growth of maize seedlings was more severe than that of its S-form (Zhou et al., 2009). Cis-bifenthrin selectively induced oxidative damage and DNA damage in a human amnion epithelial (FL) cell line, which led to cytotoxicity (Liu et al., 2008). Ma et al. reported that αS-2S-fenvalerate caused significant emergence of zebrafish crooked body, yolk sac edema, and pericardial edema, further reporting that the 96-h mortality was 3.8 times higher than those of the other isomers (Ma et al., 2009).

Currently, several studies regarding the enantioselective separation, degradation, and enantioselective fungicidal activity and toxicity related to TRZ have been published. Chromatographic separation methods mainly include liquid chromatography-tandem mass spectrometry (LC-MS/MS) (Chai et al., 2014; Zhang et al., 2018b) and supercritical fluid chromatography (SFC) (Jiang et al., 2018; Tan et al., 2017), which have been used for the enantioseparation of TRZ. Zhang et al. studied the fungicidal activity of TRZ on nine phytopathogens, and found that the fungicidal activity of S-TRZ was lower than that of R-TRZ. Moreover, the R-form inhibited cell membrane synthesis and ergosterol biosynthesis 1.80–7.34 times more than its enantiomer. Zhang et al. further reported that the degradation of two enantiomers was also stereoselective. (R)-TRZ was less persistent than (S)-TRZ in spinach, pakchoi, tomato, and cucumber under field conditions (Zhang et al., 2018a). Nie et al. studied the toxicokinetics of TRZ enantiomers in rats. After single oral administration of 50 mg/kg racemic TRZ (rac-TRZ) to rats, the $AUC_{(0-\infty)}$ and C_{max} of R-(−)-TRZ were 3.5 and 3.6 times higher than that of S-(+)-TRZ, respectively. The content of S-(+)-TRZ was higher in the kidney whilst the content of R-(−)-TRZ was higher in the brain and small intestine (Nie et al., 2019). A study of the enantioselective accumulation of TRZ in the earthworm *Eisenia fetida* showed that its bioaccumulation was enantioselective and R-TRZ was preferentially accumulated (Wang et al., 2019). However, few studies investigated the toxicity of TRZ to aquatic organisms, neither of which investigated stereoselectivity (de Albuquerque et al., 2018).

Since excessively applied pesticides dissolve in water or are adsorbed by soil particles, they may be easily transported to the aquatic environment through run-off surface water. Numerous non-target aquatic microalgae may be exposed to a variety of toxic effects, such as photosynthetic inhibition and growth-related metabolic processes (Coogan et al., 2007; Kümmerer, 2009).

As a primary producer, green algae play an important role in the aquatic ecosystem. Due to their high sensitivity to pollutants in the water, they are widely used to assess the quality of the aquatic environment (Camuel et al., 2017; Iswarya et al., 2017). Pigments, lipid peroxides, and antioxidant enzyme activities in algae vary in response to the level of pesticides in the water (Geoffroy et al., 2002). Liu et al. reported that the activities of antioxidant enzymes (superoxide dismutase (SOD), catalase (CAT), ascorbate peroxidase (APX), glutathione peroxidase (GPX), peroxidase (POD)) and the content of malondialdehyde (MDA) in *Chlorella vulgaris* increased significantly after exposure to rac-paclobutrazol and its enantiomers (1, 5, and 10 mg/L) for 96 h (Liu et al., 2019). After 96 h exposure to triflumizole (0.2 and 1 mg/L), the chlorophyll content (chlorophyll a, chlorophyll b, and total chlorophyll) of *C. vulgaris* had significantly decreased compared with control. In addition, the contents of reactive oxygen species (ROS) and MDA as well as the activities of antioxidant enzymes (such as SOD and CAT) in algal cells increased. Furthermore, the activities of antioxidant enzymes and the contents of ROS and MDA increased with increasing pesticide concentration (Xi et al., 2019).Therefore, it is significant to study the effects of chiral pesticides on algae.

Under various environmental stresses, lipid droplets (LDs) form rapidly in algal cells (Zienkiewicz et al., 2016). Microalgal lipids consist of polar lipids and neutral lipids. Under optimal growth conditions, microalgal cells primarily synthesize polar lipids (including glycolipids) for chloroplast membranes of photosynthetic microalgae as well as phospholipids for plasma and many membranes of organelles (Guckert and Cooksey, 1990). Under pressure, the lipid biosynthesis pattern of microalgae changes, neutral lipids accumulate to form lipid droplets that are located in the cytoplasm, the main form of which is triacylglycerol (TAG) (Wang et al., 2009). Excessive ROS may stimulate *de novo* synthesis of TAG. Previous studies have shown that *Chlamydomonas* produced TAG in stressful environments, e.g. in response to high salinity (Siaut et al., 2011), iron deficiency (Urzica et al., 2013), nitrogen (N) depletion (Siaut et al., 2011), or high temperature (Légeret et al., 2016). Few studies reported the effect of pesticide exposure on lipid synthesis in algae; therefore, it makes sense to determine the TAG content after exposure to TRZ.

In the present study, *C. pyrenoidosa* was exposed to TRZ for 96 h to determine the 96h-EC_{50} values of racemate and enantiomers against *C. pyrenoidosa*. Furthermore, the content of ROS in *C. pyrenoidosa* was determined. The ultrastructure of algal cells was observed and the contents of photosynthetic pigments were measured to explore the effects of TRZ on the photosynthetic systems of algal cells. For the antioxidant system and lipid accumulation, SOD and CAT activities were measured, as well as MDA, nicotinamide adenine dinucleotide (NADH),

and TAG contents in algal cells after 96 h of exposure. The results enable a better understanding of the enantioselective toxic effects and enantioselective toxic mechanisms of TRZ to *C. pyrenoidosa*.

2. Materials and methods

2.1. Chemicals and reagents

Analytical-grade racemate and two enantiomers of TRZ were provided by the School of chemistry and environment, South China Normal University, China, and were verified by high performance liquid chromatography (HPLC). Identification was conducted as described in the Supplementary material.

All other analytical-grade reagents in this study were purchased from Yili Fine Chemicals (Beijing, China). Water was purified with a Milli-Q system (Millipore Purification Systems). TRZ and its two enantiomers were dissolved in dimethyl sulfoxide (DMSO).

2.2. Algal culture

Chlorella pyrenoidosa was obtained from the Institute of Hydrobiology, Chinese Academy of Science (Wuhan, China). Before the assay, *C. pyrenoidosa* were cultivated in sterile 250 mL flasks, containing 100 mL of liquid sterile BG-11 medium under standard temperature and light conditions (12:12 light:dark cycle; 70 μmol photons/m^2/s; 25 °C), and stored in an environmental chamber. BG-11 medium was prepared as described in the supplementary material.

2.3. Algal growth inhibition test

An algal growth inhibition test was conducted to determine the effects of rac-, R-(−)-, (S)-(+)- TRZ on the growth of *C. pyrenoidosa* according to the updated OECD guideline 201 (OECD, 2011). *C. pyrenoidosa* cells were pre-cultured until the exponential growth phase. Based on the results of a preliminary experiment, the growth test was conducted under different concentrations (0.1, 1, 12, 20, 30, and 40 mg/L for (S)-(+)-TRZ; 0.05, 0.1, 1, 4, 8, and 12 mg/L for R-(−)-TRZ and racemate). The DMSO concentration of the medium was below 0.1% v/v. The initial cell density was 200,000 cells/mL, and controls were grown in the absence of fungicides. Each assay was performed in triplicate. The flasks were incubated under the conditions described above, and each flask was shaken three times daily to prevent cell caking. Densities of algal suspensions were measured after 96 h by measuring the optical density at 650 nm (OD_{650}) to obtain the cell density. The resulting inhibition of algal growth was calculated by normalizing the data to the results of control cultures (OECD, 2011).

2.4. Determination of photosynthetic pigment content

Due to the significant differences in the 96-h EC_{50} value of TRZ racemate and enantiomers to *C. pyrenoidosa*, algal cells were exposed to 0.1 mg/L, 1 mg/L, and 4 mg/L of rac- and R-(−)-TRZ, and 1 mg/L, 20 mg/L, and 30 mg/L of (S)-(+)-TRZ for 96 h to measure the pigment contents.

The contents of photosynthetic pigments were measured as described by Ritchie (2008). After exposure to the above treatment group, algal suspensions (5 ml) were collected after 96 h and centrifuged at 12,000 rpm for 10 min. The resulting pellet was transferred into 2 mL of ice-cold 80% acetone and extracted at 4 °C in the dark for one day. The mixture was then centrifuged at 12,000 rpm for 10 min, the supernatant was collected, and the optical density was measured at 440 nm, 645 nm, 652 nm, and 663 nm. The contents of chlorophyll a (C_a), chlorophyll b (C_b), total chlorophyll (C_T), and carotenoids (C_k) were calculated as follows (Jeffrey and Humphrey, 1975):

$$C_a = (12.7OD_{663} - 2.69OD_{645})/\rho$$

$$C_b = (22.9OD_{645} - 4.68OD_{663})/\rho$$

$$C_T = (1000OD_{652}/34.5)/\rho$$

$$C_k = (4.7OD_{440} - 0.27C_{a+b})/\rho$$

Where ρ represents the density of algal suspension (cell number/mL).

2.5. Ultrastructure of algal cells

Suspensions of *C. pyrenoidosa* were centrifuged at 3000 g for 10 min, and algal cells were collected and fixed with 2% glutaraldehyde for 24 h at 4 °C.

According to Gong et al., algal cells were exposed to 1 mg/L of TRZ for 96 h and were observed via transmission electron microscopy (TEM) (Gong et al., 2015).

2.6. Preparation of protein extracts

To better explore the enantioselective toxicity of the chiral fungicide TRZ to *C. pyrenoidosa*, *C. pyrenoidosa* was exposed to 1 mg/L of racemate and two enantiomers of TRZ. After 96 h, differently treated algal cells were collected for the determination of indicators such as ROS, SOD, CAT, MDA, NADH, and TAG.

The total protein content of *C. pyrenoidosa* was measured according to the method of Bradford (1976). Measurements were performed as described in the supplementary material.

2.7. Determination of reactive oxygen species

The intracellular ROS contents were measured based on the method of Wang and Joseph (1999). The cell permeability indicator H_2DCFDA was hydrolyzed by cell esterase to form non-fluorescent 2′,7′-dichlorodihydrofluorescein (H_2DCF) after penetrating the cells of *C. pyrenoidosa*. Then, in the presence of ROS, H_2DCF is immediately converted to the highly fluorescent 2′,7′-dichlorofluorescein (DCF) (Wang et al., 2011). DCF can be observed in a fluorescence spectrophotometer due to its the fluorescence characteristics, and its fluorescence intensity is proportional to the level of intracellular ROS.

2.8. Determination of antioxidant enzyme activities and malondialdehyde content

Algal suspensions were collected after exposure to TRZ for 96 h, and measurements were performed as described in the supplementary material.

2.9. Determination of NADH and TAG

After exposure to the racemate and enantiomers of TRZ, the *C. pyrenoidosa* suspension was diluted with phosphate buffer (pH 7.2–7.4) until the cell concentration reached about 1,000,000 cell/ml. Via repeated freezing and thawing, cell membranes were disrupted, and the intracellular components were released. The disrupted cells were then centrifuged at 30,000 rpm for 20 min. The supernatant was carefully collected for the determination of the NADH content. The NADH content of *C. pyrenoidosa* was determined by a microbial reduction coenzyme I (NADH) enzyme-linked immunosorbent assay (ELISA) kit (Shanghai Enzyme-linked Biotechnology Co., Ltd., Shanghai, China). Measurements were performed as described in the supplementary material.

TAG contents were measured according to the glycerol phosphate oxidase and peroxidase (GPO-PAP) method (Henkel and Stoltz, 1982). Free glycerol was removed from the reaction mixture by pre-incubation with glycerol phosphate oxidase and peroxidase. Subsequently, lipase and the chromogen, 4-aminoantipyrine were added, which resulted in the formation of color proportional to the amount of triglycerides (Sullivan et al., 1985). The TAG content was determined by a TAG test

Table 1
96h-EC_{50} values of rac-triticonazole and its enantiomers against *C. pyrenoidosa*.

Compound	EC_{50}(mg/L) [a]	Confidence intervals(mg/L)[b]	R^{2}[c]
Rac-triticonzole	1.939	1.625–2.226	0.932
(S)-(+)-triticonazole	22.002	20.661–23.344	0.949
(R)-(−)-triticonazole	0.853	0.784–0.922	0.909

[a] EC_{50}: the effective concentration that results in a 50% reduction in population growth relative to the control.
[b] 95% confidence intervals.
[c] Correlation coefficient.

kit (Nanjing Jiancheng Bioengineering Research Institute, Nanjing, China).

2.10. Data analysis

Data were analyzed using SPSS 21.0 (SPSS, USA). All experimental response variables are expressed as means ± standard deviations (SD). Differences between control and treatments were analyzed by analysis of variance (ANOVA) followed by Student–Newman–Keuls (SNK) post-hoc analyses. The means were considered significantly different at $P < 0.05$. EC_{50} and associated 95% confidence intervals were calculated using a probit equation (Table 1).

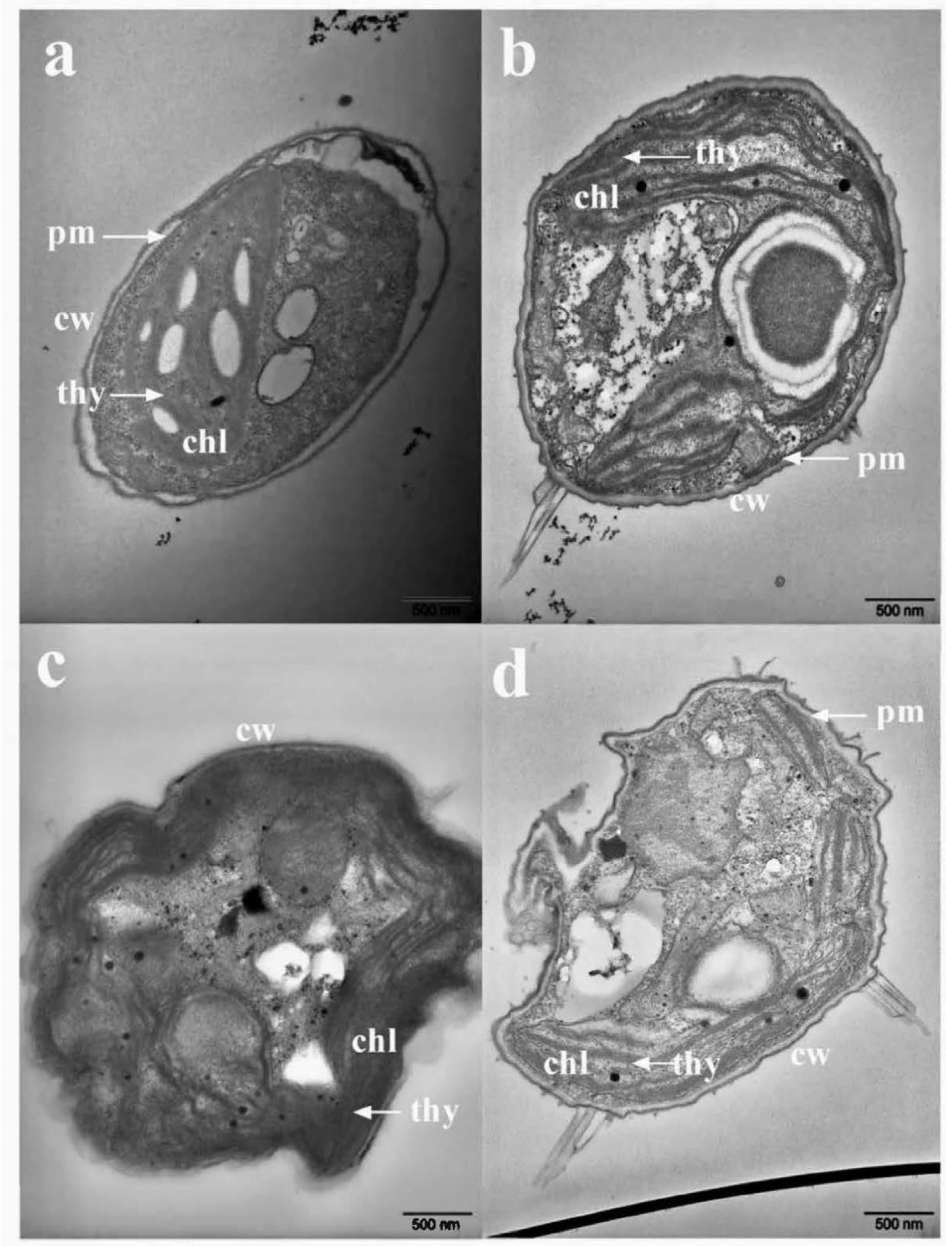

Fig. 2. TEM Photomicrographs of *C. pyrenoidosa* cells after 96 h of growth. a: control; b: (S)-(+)-triticonazole, c: (R)-(−)-triticonazole; d: rac-triticonazole. cw, cell wall; pm, plasma membrane; chl, chloroplast; thy, thylakoids.

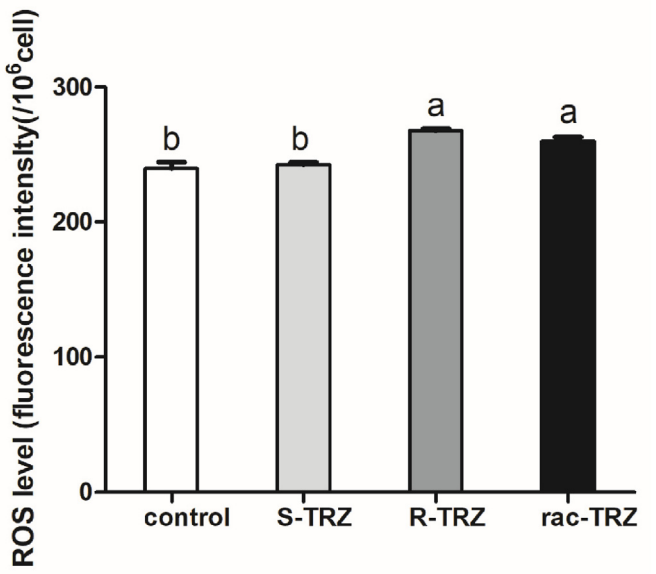

Fig. 3. ROS level in *C. pyrenoidosa* after exposed to racemate and enantiomers of triticonazole (TRZ) at 1 mg/L after 96 h different letters represent statistically significant different between control and treatments at $P < 0.05$.

3. Results and discussion

3.1. 96h-EC_{50} value of triticonazole to C. pyrenoidosa

The EC_{50} value is a sensitive index for the evaluation of the toxicity of compounds, and a higher value indicates lower toxicity (Zhang et al., 2016). Therefore, EC_{50} was chosen as an indicator to investigate the enantioselective acute toxicity of TRZ racemate and enantiomers on *C. pyrenoidosa* growth for 96 h. Details regarding the calculation are provided in the supplementary material. EC_{50} values (the concentration that reduces the population growth rate by 50%) were greatly different between the 96-h acute toxicity of rac-TRZ and a pair of enantiomers toward *C. pyrenoidosa* (Table 1). The EC_{50} value of rac-TRZ was 1.939 mg/L. The (S)-(+)-enantiomer posed lower toxicity to *C. pyrenoidosa* with an EC_{50} value of 22.002 mg/L, and (R)-(−)-TRZ was more toxic with an EC_{50} value of 0.853 mg/L. The 96-h EC_{50} value of (S)-(+)-TRZ to *C. pyrenoidosa* was about 26 times higher than that of the (R)-enantiomer. This showed that *C. pyrenoidosa* was more sensitive to (R)-(−)-TRZ than (S)-(+)-TTRZ during the exposure time. In brief, after 96 h of exposure, the order of acute toxicity to *C. pyrenoidosa* cells followed: (R)-(−)-TRZ > rac-TRZ > (S)-(+)-TRZ. Therefore, the acute aquatic toxicity of TRZ stereoisomers to *C. pyrenoidosa* indicated stereoselectivity. Previous studies reported the enantioselective toxicity of triazole fungicides to organisms. For example, Zhang et al. (2015) studied the biological activity of flutriafol enantiomers against *Rhizoctonia solani*, *Alternaria solani*, *Pyricularia grisea*, *Gibberella zeae*, and *Botrytis cinerea*. The results showed that the R-flutriafol fungicidal activity was higher than that of its enantiomer. R-flutriafol was 2.17–3.52 times more toxic than its S-form to *Eisenia fetida* and *Scenedesmus obliquus*. Li et al. studied the enantioselectivity of myclobutanil and tebuconazole and evaluated the acute toxicity to *Daphnia magna*, *Scenedesmus obliquus*, and *Danio rerio*. The results showed that the toxicity of R-(−)-tebuconazole was about 1.4–5.9 times higher than that of its S-form, and rac-myclobutanil was about 1.3–6.1 and 1.4–7.3 more toxic than (−)-myclobutanil and (+)-myclobutanil, respectively (Li et al., 2015). Therefore, enantioselective toxicity should be considered when evaluating the influence of chiral compounds to aquatic organisms.

3.2. Effects of triticonazole on the ultrastructure of algal cells

The ultrastructure of *C. pyrenoidosa* cells was examined to study the changes of cell and chloroplast structure after TRZ treatment at 1 mg/L (Fig. 2).

In control samples, cells were structurally intact, the plasma membrane was close to the cell wall, the chloroplast structure was intact, and thylakoid lamellae were correctly arranged (Fig. 2a). After exposure to 1 mg/L of (S)-(+)-TRZ for 96 h, cells showed slightly swollen thylakoids while the internal structure of *C. pyrenoidosa* cells did not change significantly compared with control; moreover, cells maintained normal morphology (Fig. 2b). After exposure to 1 mg/L of racemate and (R)-(−)-TRZ, thylakoids were strongly swollen and cells did not maintain their normal spherical shape (Fig. 2c and d). Especially after exposure to (R)-(−)-TRZ, the cell membrane shrank severely, organelles dissolved, cytoplasm leaked, and the thylakoid structure was severely damaged, all of which affected the normal function of the chloroplast (Fig. 2c). The thylakoid contains the photosynthetic pigments, reaction centers, and the electron-transport chain, and it is the place of the light-photosynthetic reactions (Strašková, 2019). Damage to the thylakoid structure will inevitably affect the normal photosynthesis process (Deng et al., 2019).

In plant cells, ROS are produced in chloroplasts and mitochondria by the electron transport system (Schippers et al., 2008). The ultrastructure of algal cells demonstrated enantioselective effects of these enantiomers on the chloroplast structure and cell morphology of *C. pyrenoidosa*. (R)-(−)-enantiomer selectively affected the normal transmission of electrons and generated excessive electrons, resulting in a considerable production of ROS, thus disrupting the thylakoid structure and cell integrity, and affecting the photosynthetic process of *C. pyrenoidosa*.

3.3. Effects of triticonazole on algae physiological and biochemical indexes

Under adverse conditions, such as drought, heavy metal exposure, and pesticide exposure, *C. pyrenoidosa* may respond with a pronounced burst of ROS (Collén et al., 1994; Küpper et al., 2001). Excessive amounts of ROS react with critical cellular molecules such as proteins, lipids, nucleic acids, and pigments, thus disrupting cellular functions (Bali and Sidhu, 2019).

After algae were exposed to 1 mg/L of TRZ racemate and enantiomers, the order of ROS content in *C. pyrenoidosa* followed: control < (S)-(+)-TRZ < rac-TRZ < (R)-(−)-TRZ (Fig. 3). Especially in the (R)-(−)-TRZ treatment group, the ROS content of *C. pyrenoidosa* was 108.41% of that of the control group, indicating that the (R)-(−)-enantiomer caused an imbalance between the production and elimination of ROS in algal cells, which resulted in excessive ROS accumulation. The same concentration of enantiomers exerted different effects on the accumulation of ROS in algal cells, which showed certain enantioselectivity. The ROS content of the (S)-(+)-enantiomer treatment group was not significantly different from that of the control group. However, after exposure to (R)-(−)-TRZ, a large amount of ROS was produced by algal cells.

Antioxidant defense mechanisms protect plants against damage due to oxidative stress (Gill and Tuteja, 2010). SOD and CAT are important enzymes that are related to antioxidant stress in plants (Wan et al., 2014). SOD and CAT cooperate to resist oxidative stress, and remove ROS caused by toxic substances to protect the normal biological homeostasis (Balaban et al., 2005). In plants, SOD is the first line of defense against oxidation, which involves the conversion of superoxide radicals (O^{2-}) to O_2 and hydrogen peroxide (H_2O_2) (Fridovich, 1995). CAT catalyzes the degradation or reduction of H_2O_2 to water and oxygen molecules, thus further protecting cells and tissues from oxidative damage (Chelikani et al., 2004; Marklund, 1984).

As shown in Fig. 4, after exposure to 1 mg/L TRZ racemate and enantiomers, SOD and CAT activities significantly increased in *C.*

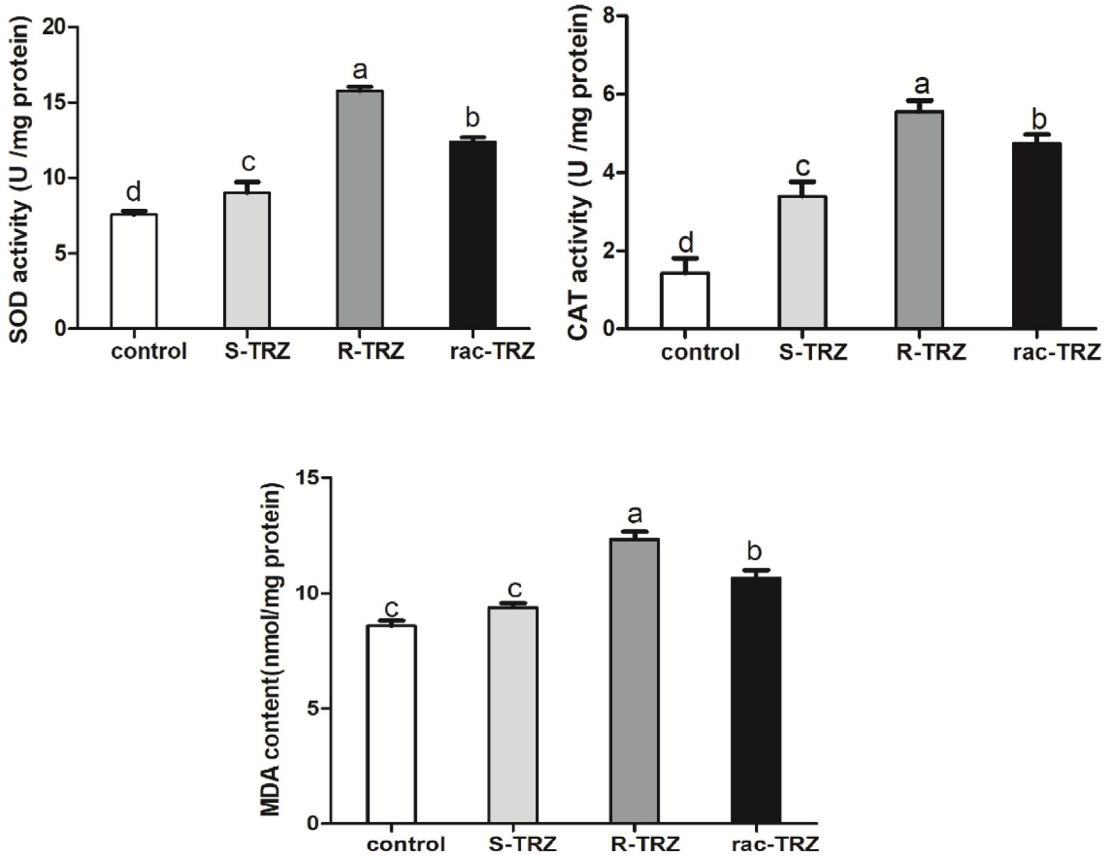

Fig. 4. SOD,CAT activity and MDA content in *C. pyrenoidosa* after exposed to racemate and enantiomers of triticonazole (TRZ) at 1 mg/L after 96 h different letters represent statistically significant different between control and treatments at $P < 0.05$.

pyrenoidosa compared with the control group. The high activities of SOD and CAT may be due to the overproduction of superoxide, resulting in increased expression of genes encoding SOD and CAT or in activation of existing enzyme pools (Foyer et al., 1997; Mishra et al., 2006; Xie et al., 2011). The order of SOD and CAT activities in *C. pyrenoidosa* was consistent with ROS content and followed: control < (S)-(+)-TRZ < rac-TRZ < (R)-(−)-TRZ. Both antioxidant enzyme activities were highest after exposure to (R)-(−)-TRZ. This indicates that algae exposed to (R)-(−)-enantiomer suffered higher oxidative stress than other treatments, and antioxidant enzymes were highly activated to remove excessive ROS.

The structure of intracellular membranes is composed of unsaturated phospholipids, which are easily attacked by free oxygen radicals, thus leading to MDA accumulation (Hong et al., 2008; Qian et al., 2009b, 2009c). MDA is one of the final products of lipid oxidative degradation and has been used as a marker for lipid peroxidation, since it reflects the cellular lipid oxidative damage under environmental stress conditions.

After 96 h of exposure to 1 mg/L TRZ (with the exception of the (S)-(+)-enantiomer), the MDA content of *C. pyrenoidosa* treated with the other two compounds increased significantly (Fig. 4). The MDA content of algal cells exposed to (R)-(−)-enantiomer increased significantly, and was 143.97% higher than that of the control. This indicates that the antioxidant defense system of *C. pyrenoidosa* failed to effectively eliminate the vast amount of ROS produced by (R)-(−)-TRZ stress, and the excessive ROS caused severe lipid oxidative damage in algal cells.

Excessive accumulation of ROS can also decompose indole-3-acetic acid (IAA), desrupt the pigment system of photosynthesis, and irreversibly destroy lipids, proteins, and DNA, thus leading to the disruption of normal cell function (Boonstra and Post, 2004).

After exposure to TRZ, the chlorophyll a and total chlorophyll content of algal cells decreased significantly in all treatment groups compared with control (Fig. 5a). Moreover, the contents of photosynthetic pigments were basically dose-dependent. With increasing pesticide concentration, the pigment content of *C. pyrenoidosa* decreased gradually. Compared with the control, in the highest concentration exposure group of (S)-(+)-, (R)-(−)-, and rac-TRZ, the C_a content decreased by 89.20%, 62.30%, and 59.03%; the C_b content decreased by 68.72%, 61.20%, and 49.30%; the C_k content decreased by 74.29%, 58.11%, and 51.05%; and the C_T content decreased by 73.27%, 61.89%, and 60.05%, respectively. This decrease in photosynthetic pigment contents may be due to stress-induced damage to the pigment biosynthetic pathway or pigment degradation (Misra et al., 1998). Moreover, the destruction of the structure of the thylakoid membrane may also result in damage of the chlorophyll binding state, thus inhibiting the absorption, transmission, and distribution of light energy by the thylakoid membrane (Janik et al., 2013).

It is worth noting that at a concentration of 1 mg/L, the effects of TRZ racemate and enantiomers on the pigments of *C. pyrenoidosa* were different. (R)-(−)-TRZ inhibited the synthesis of Chlorella pigments significantly. However, at the same concentration, (S)-(+)-enantiomer exerted little effect on pigments (Fig. 5b). The impact of rac-TRZ on the pigment content of algal cells ranged between the effects of both enantiomers. Based on the EC_{50} value, the concentration of 1 mg/L was closed to the 96h-EC_{50} value of (R)-(−)-, and rac-TRZ to *C. pyrenoidosa*, but much lower than the EC_{50} value of the (S)-(+)-enantiomer.

The effects of 1 mg/L TRZ on photosynthetic pigments in *C. pyrenoidosa* were enantioselective. Compared with other treatment groups, the four pigment contents in the (R)-(−)-enantiomer treatment group were lowest. The reason may be that (R)-(−)-TRZ produced severe

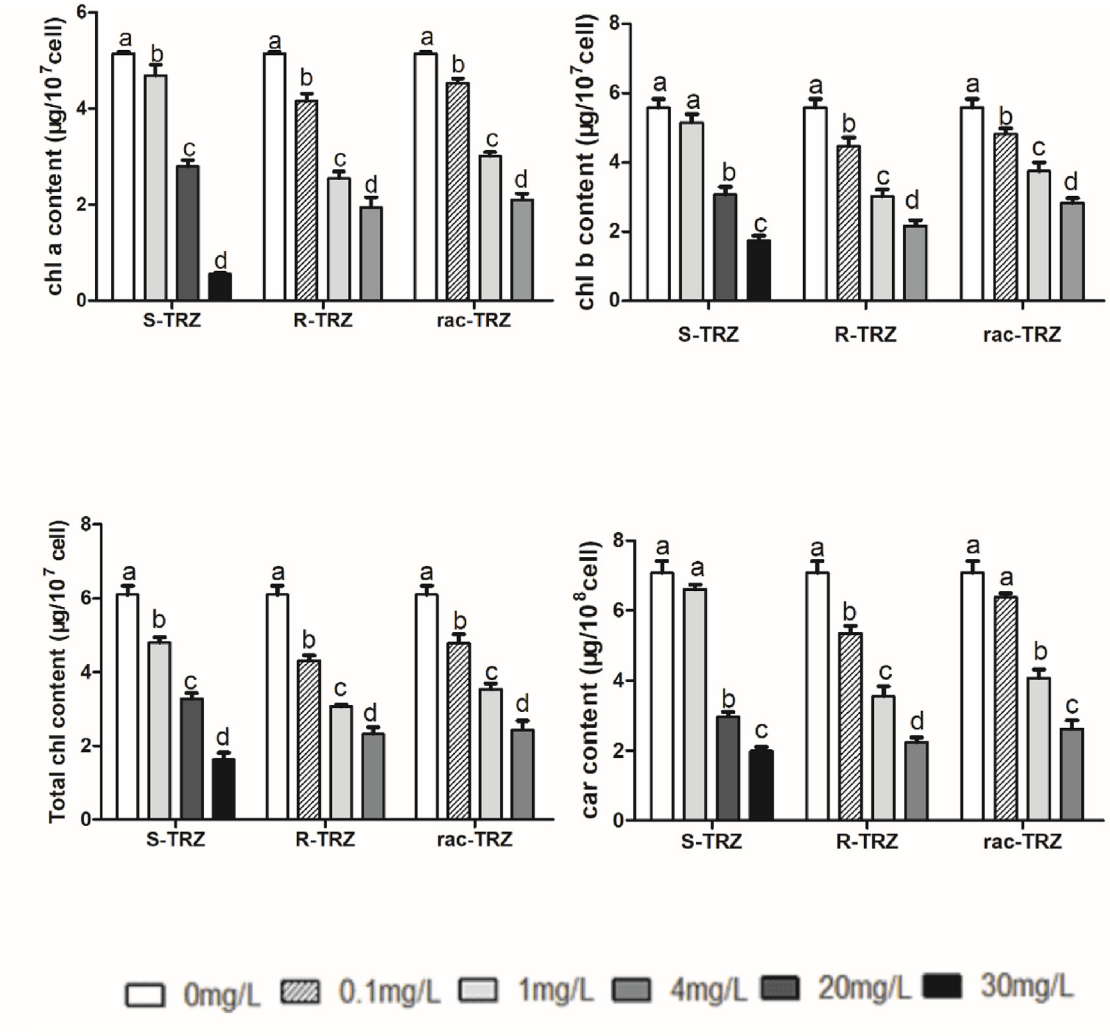

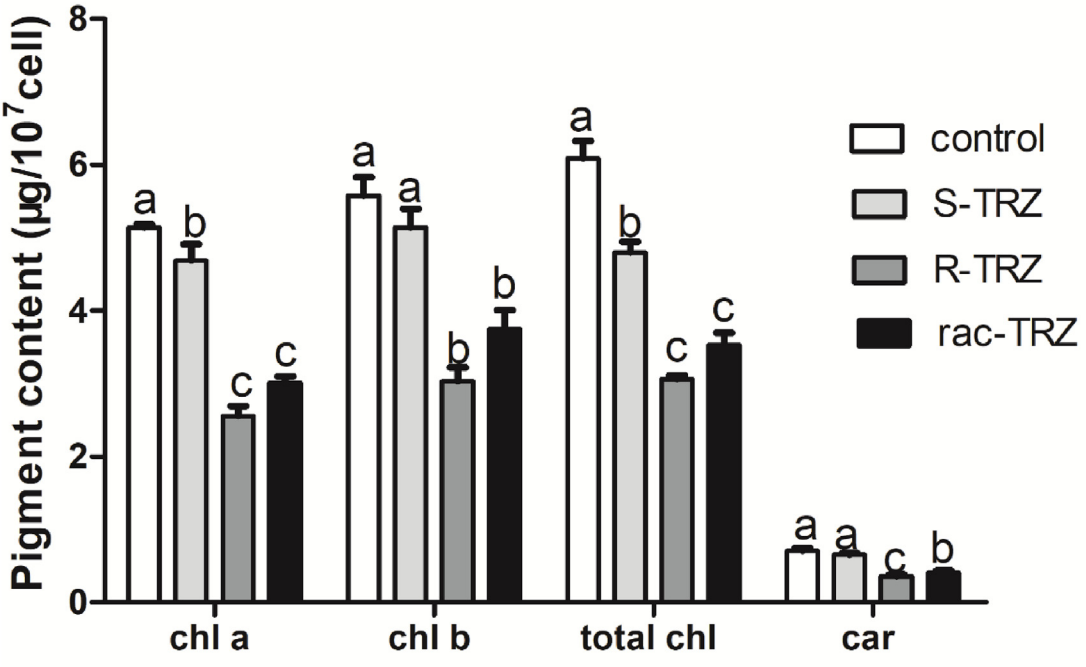

Fig. 5. a. Contents of photosynthetic pigments in *C. pyrenoidosa* after 96 h of exposure to different doses and forms of triticonazole (TRZ).different letters represent statistically significant different between control and treatments at $P < 0.05$. b. Contents of pigments in *C. pyrenoidosa* after 96 h of exposure to 1 mg/L different forms of triticonazole (TRZ).different letters represent statistically significant different between control and treatments at $P < 0.05$.

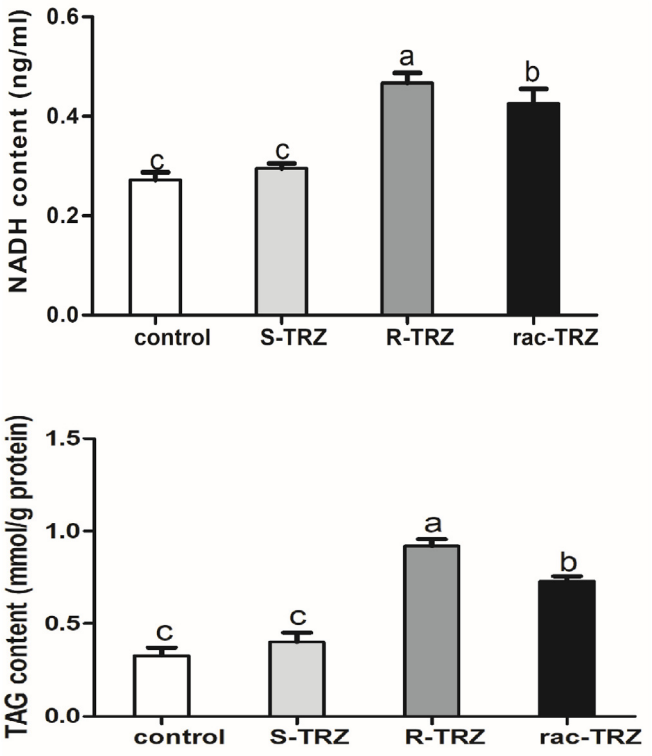

Fig. 6. Effects of 1 mg/L rac-triticonazole (TRZ) and its enantiomers on the accumulation of NADH and TAG in *C. pyrenoidosa* after 96 h of exposure. different letters represent statistically significant different between control and treatments at $P < 0.05$.

abiotic stress on *C. pyrenoidosa*, thus causing excessive ROS accumulation, which significantly inhibited chlorophyll synthesis. Moreover, the (R)-(−)-enantiomer selectively destroyed the chloroplast structure of algal cells (Fig. 2), which led to the destruction of the chlorophyll-binding state, which ultimately affected the normal photosynthetic process of algal cells.

It is generally believed that lipids in algal cells exert a protective role in response to environmental stimuli. Lipids are considered as an electron sink and a secondary storage compound to prevent excessive production of ROS caused by excessive electrons produced by photosynthesis (Hu et al., 2008).

It has been reported that many species of microalgae accumulate a large number of TAG under conditions such as nutrient deficiency, extreme temperature, and high salinity (Guschina and Harwood, 2006). However, few studies have investigated the effects of pesticides on the accumulation of triglycerides in microalgae.

Fig. 6 showed that large amounts of NADH and TAG accumulated in cells after exposure to 1 mg/L of (R)-(−)-TRZ for 96 h. Compared with the control group, (S)-(+)-TRZ did not significantly increase the NADH and TAG contents in *C. pyrenoidosa*. Exposure to 1 mg/L of (R)-(−)-TRZ caused a substantial accumulation of TAG in *C. pyrenoidosa* cells, which was 280.76% of that of the control group. After 96 h of exposure to TRZ, the order of NADH and TAG contents in *C. pyrenoidosa* cells was (R)-(−)-TRZ > rac-TRZ > (S)-(+)-TRZ > control.

NADH is the electron donor of the photosynthetic system at the plastoquinone functional site (Godde and Trebst, 1980). Damage to the photosynthetic machinery under stress conditions increased the concentration of NADH (Nanda et al., 2019). High NADH concentrations indicate a high energy supply for the cells, which inhibits the enzyme citrate synthetase and prevents acetyl CoA from entering the TCA cycle to produce energy. This would result in the increase in acetyl CoA levels, which is then converted to malonyl CoA, which ultimately initiates TAG accumulation (Praveenkumar et al., 2012). The synthesis of TAG sequesters the overabundance of electrons from photosynthesis and functions as an electron sink, which safeguards the thylakoid membrane by releasing ROS (Ibrahim et al., 2014; Iwai et al., 2014). TAG acts as energy storage and thus contributes to the survival of microalgae during stress (Rabbani et al., 1998; Zhekisheva et al., 2002).

Combined with other results, it could be concluded that (R)-(−)-TRZ posed high 96-h toxicity to *C. pyrenoidosa*, and caused severe stress on algal cells, which resulted in a large accumulation of ROS. Excessive ROS caused severe damage to the photosynthetic system of *C. pyrenoidosa*, thus stimulating a notable accumulation of NADH and TAG to resist external stress.

4. Conclusion

The presented results showed that the 96-h acute toxicity of (R)-(−)-TRZ against *C. pyrenoidosa* was higher than that of its (S)-(+)-enantiomer. Furthermore, (R)-(−)-TRZ stimulated excessive ROS production, and was accompanied by a significant increase in antioxidant enzymes activities and MDA content. In the (R)-(−)-enantiomer treatment group, photosynthetic pigment contents were significantly decreased and the chloroplast structure of algal cells was severely damaged. This indicates that the photosynthetic system was severely affected by exposure to (R)-(−)-TRZ. (R)-(−)-TRZ also affected lipid synthesis, resulting in the significant accumulation of NADH and TAG. In contrast, no significant difference was found in the above physiological and biochemical indexes between the (S)-(+)-enantiomer treatment group and control. This indicates that R-(−)-TRZ selectively affected photosynthetic system, antioxidant system, and lipid synthesis of algae cells, thus causing enantioselective toxic effects to *C. pyrenoidosa*.

TRZ therefore exerts enantioselective toxicity to non-target organisms, indicating that the use of its racemate may cause unpredictable environmental damage. Therefore, to reduce the hidden dangers of chiral pesticides for the ecological environment, the environmental risk of TRZ should be evaluated at the stereoselective level. It is also necessary to study the fungicidal activity of TRZ racemate and enantiomers and their effects on the growth of target crops to comprehensively evaluate and correctly use TRZ and minimize the negative impact of chiral pesticides on the environment. This will be addressed by our future research.

Acknowledgements

This work was supported by the National Natural Science Foundation of China (Contract grant number: 21577171) and the National Key Research and Development Program of China (2016 YFD 0200202).

Appendix A. Supplementary data

Supplementary data to this article can be found online at https://doi.org/10.1016/j.ecoenv.2019.109691.

References

Balaban, R.S., et al., 2005. Mitochondria, oxidants, and aging. Cell 120, 483–495.
Bali, A.S., Sidhu, G.P.S., 2019. Abiotic stress-induced oxidative stress in wheat. In: Hasanuzzaman, M. (Ed.), Wheat Production in Changing Environments: Responses, Adaptation and Tolerance. Springer Singapore, Singapore, pp. 225–239.
Boonstra, J., Post, J.A., 2004. Molecular events associated with reactive oxygen species and cell cycle progression in mammalian cells. Gene 337, 1–13.
Bradford, M.M., 1976. A rapid and sensitive method for the quantitation of microgram quantities of protein utilizing the principle of protein-dye binding. Anal. Biochem. 72, 248–254.
Burden, R.S., et al., 1987. Comparative activity of the enantiomers of triadimenol and paclobutrazol as inhibitors of fungal growth and plant sterol and gibberellin biosynthesis. Pestic. Sci. 21, 253–267.
Camuel, A., et al., 2017. Fast algal eco-toxicity assessment: influence of light intensity and

exposure time on Chlorella vulgaris inhibition by atrazine and DCMU. Ecotoxicol. Environ. Saf. 140, 141–147.
Chai, T., et al., 2014. Simultaneous stereoselective detection of chiral fungicides in soil by LC–MS/MS with fast sample preparation. J. Sep. Sci. 37, 595–601.
Chelikani, P., et al., 2004. Diversity of structures and properties among catalases. Cellular and Molecular Life Sciences CMLS 61, 192–208.
Collén, J., et al., 1994. A stress-induced oxidative burst in Eucheuma platycladum (Rhodophyta). Physiol. Plant. 92, 417–422.
Coogan, M.A., et al., 2007. Algal bioaccumulation of triclocarban, triclosan, and methyltriclosan in a North Texas wastewater treatment plant receiving stream. Chemosphere 67, 1911–1918.
Davis, T.D., et al., 1988. Triazole plant growth regulators. Hortic. Rev. 10, 63–103.
de Albuquerque, N.C.P., et al., 2018. Metabolism studies of chiral pesticides: a critical review. J. Pharm. Biomed. Anal. 147, 89–109.
Deng, Y., et al., 2019. Stereoselective toxicity of metconazole to the antioxidant defenses and the photosynthesis system of Chlorella pyrenoidosa. Aquat. Toxicol. 210, 129–138.
Fletcher, R.A., 1988. Triazoles as potential plant protectants. Sterol Biosynthesis Inhibitors : Pharmaceutical and Agricultural aspects 321–331.
Foyer, C.H., et al., 1997. Hydrogen peroxide- and glutathione-associated mechanisms of acclimatory stress tolerance and signalling. Physiol. Plant. 100, 241–254.
Fridovich, I., 1995. Superoxide radical and superoxide dismutases. Annu. Rev. Biochem. 64, 97–112.
Geoffroy, L., et al., 2002. Effect of oxyfluorfen and diuron alone and in mixture on antioxidative enzymes of Scenedesmus obliquus. Pestic. Biochem. Physiol. 72, 178–185.
Gill, S.S., Tuteja, N., 2010. Reactive oxygen species and antioxidant machinery in abiotic stress tolerance in crop plants. Plant Physiol. Biochem. 48, 909–930.
Godde, D., Trebst, A., 1980. NADH as electron donor for the photosynthetic membrane of Chlamydomonas reinhardii. Arch. Microbiol. 127, 245–252.
Gong, Y., et al., 2015. Vernalophrys algivore gen. Nov., sp. nov. (rhizaria: Cercozoa: Vampyrellida), a new algal predator isolated from outdoor mass culture of Scenedesmus dimorphus. Appl. Environ. Microbiol. 81, 3900–3913.
Guckert, J.B., Cooksey, K.E., 1990. Triglyceride accumulation and fatty acid profile changes in chlorella (Chlorophyta) during high pH-induced cell cycle inhibition1. J. Phycol. 26, 72–79.
Guschina, I.A., Harwood, J.L., 2006. Lipids and lipid metabolism in eukaryotic algae. Prog. Lipid Res. 45, 160–186.
Henkel, E., Stoltz, M., 1982. A newly drafted colour test for the determination of triglycerides convenient for manual and mechanized analysis (glycerolphosphate-oxidase — PAP method). Fresenius' Z. für Anal. Chem. 311, 451–452.
Hong, Y., et al., 2008. Physiological and biochemical effects of allelochemical ethyl 2-methyl acetoacetate (EMA) on cyanobacterium Microcystis aeruginosa. Ecotoxicol. Environ. Saf. 71, 527–534.
Hu, F., et al., 2010. Enantioselective induction of oxidative stress by permethrin in rat adrenal pheochromocytoma (PC12) cells. Environ. Toxicol. Chem. 29, 683–690.
Hu, Q., et al., 2008. Microalgal triacylglycerols as feedstocks for biofuel production: perspectives and advances. Plant J. 54, 621–639.
Ibrahim, W.M., et al., 2014. Biodegradation and utilization of organophosphorus pesticide malathion by Cyanobacteria. BioMed Res. Int. 2014 392682-392682.
Iswarya, V., et al., 2017. Impact of tetracycline on the toxic effects of titanium dioxide (TiO2) nanoparticles towards the freshwater algal species, Scenedesmus obliquus. Aquat. Toxicol. 193, 168–177.
Iwai, M., et al., 2014. Enhancement of extraplastidic oil synthesis in Chlamydomonas reinhardtii using a type-2 diacylglycerol acyltransferase with a phosphorus starvation-inducible promoter. Plant biotechnology journal 12, 808–819.
Janik, E., et al., 2013. Organization and functionality of chlorophyll–protein complexes in thylakoid membranes isolated from Pb-treated Secale cereale. J. Photochem. Photobiol. B Biol. 125, 98–104.
Jeffrey, S.W., Humphrey, G.F., 1975. New spectrophotometric equations for determining chlorophylls a, b, c1 and c2 in higher plants, algae and natural phytoplankton. Biochem. Physiol. Pflanz. (BPP) 167, 191–194.
Jiang, Y., et al., 2018. High-fast enantioselective determination of prothioconazole in different matrices by supercritical fluid chromatography and vibrational circular dichroism spectroscopic study. Talanta 187, 40–46.
Kümmerer, K., 2009. Antibiotics in the aquatic environment – a review – Part I. Chemosphere 75, 417–434.
Küpper, F.C., et al., 2001. Oligoguluronates elicit an oxidative burst in the Brown algal kelp < em > Laminaria digitata < /em > Plant Physiol. 125, 278–291.
Kahle, M., et al., 2008. Azole fungicides: occurrence and fate in wastewater and surface waters. Environ. Sci. Technol. 42, 7193–7200.
Kurihara, N., et al., 1999. Chirality in synthetic agrochemicals: bioactivity and safety considerations. Pestic. Sci. 55 219-219.
Légeret, B., et al., 2016. Lipidomic and transcriptomic analyses of Chlamydomonas reinhardtii under heat stress unveil a direct route for the conversion of membrane lipids into storage lipids. Plant Cell Environ. 39, 834–847.
Li, Y., et al., 2015. Enantioselectivity in tebuconazole and myclobutanil non-target toxicity and degradation in soils. Chemosphere 122, 145–153.
Liu, C., et al., 2019. Enantioselective growth inhibition of the green algae (Chlorella vulgaris) induced by two paclobutrazol enantiomers. Environ. Pollut. 250, 610–617.
Liu, H., et al., 2008. Enantioselective cytotoxicity of the insecticide bifenthrin on a human amnion epithelial (FL) cell line. Toxicology 253, 89–96.
Ma, Y., et al., 2009. Enantioselectivity in aquatic toxicity of synthetic pyrethroid insecticide fenvalerate. Ecotoxicol. Environ. Saf. 72, 1913–1918.
Marklund, S.L., 1984. Extracellular superoxide dismutase and other superoxide dismutase isoenzymes in tissues from nine mammalian species. Biochem. J. 222, 649–655.
Mishra, S., et al., 2006. Phytochelatin synthesis and response of antioxidants during cadmium stress in Bacopa monnieri L◊. Plant Physiol. Biochem. 44, 25–37.
Misra, A.N., et al., 1998. Sodium chloride salt stress induced changes in thylakoid pigment-protein complexes, PS II activity and TL glow peaks of chloroplasts from mungbean (Vigna radiata L.) and Indian mustard (Brassica juncea Coss.) seedlings. Zeitschrift fur Naturforschung. C, Journal of biosciences. 54, 640–644.
Nanda, M., et al., 2019. Detoxification mechanism of organophosphorus pesticide via carboxylestrase pathway that triggers de novo TAG biosynthesis in oleaginous microalgae. Aquat. Toxicol. 209, 49–55.
Nie, J., et al., 2019. Development of a novel LC–MS/MS method for quantitation of triticonazole enantiomers in rat plasma and tissues and application to study on toxicokinetics and tissue distribution. J. Pharm. Biomed. Anal. 172, 78–85.
OECD, 2011. Test No. 201: Freshwater Alga and Cyanobacteria, Growth Inhibition Test, vol. 25 OECD.
Pérez-Fernández, V., et al., 2011. Chiral separation of agricultural fungicides. J. Chromatogr. A 1218, 6561–6582.
Praveenkumar, R., et al., 2012. Influence of nutrient deprivations on lipid accumulation in a dominant indigenous microalga Chlorella sp., BUM11008: evaluation for biodiesel production. Biomass Bioenergy 37, 60–66.
Qian, H., et al., 2009a. Enantioselective phytotoxicity of the herbicide imazethapyr in rice. Chemosphere 76, 885–892.
Qian, H., et al., 2009b. Combined effect of copper and cadmium on Chlorella vulgaris growth and photosynthesis-related gene transcription. Aquat. Toxicol. 94, 56–61.
Qian, H., et al., 2009c. Allelochemical stress causes oxidative damage and inhibition of photosynthesis in Chlorella vulgaris. Chemosphere 75, 368–375.
Quérou, R., et al., 1998. Uptake and fate of triticonazole applied as seed treatment to spring wheat (Triticum aestivum L.). Pestic. Sci. 53, 324–332.
Rabbani, S., et al., 1998. Induced beta-carotene synthesis driven by triacylglycerol deposition in the unicellular alga dunaliella bardawil. Plant Physiol. 116, 1239–1248.
Ritchie, R.J., 2008. Universal chlorophyll equations for estimating chlorophylls a, b, c, and d and total chlorophylls in natural assemblages of photosynthetic organisms using acetone, methanol, or ethanol solvents. Photosynthetica 46, 115–126.
Schippers, J.H.M., et al., 2008. The < em > Arabidopsis onset of leaf death5 < /em > mutation of quinolinate synthase affects nicotinamide adenine dinucleotide biosynthesis and causes early ageing. The Plant Cell 20, 2909–2925.
Siaut, M., et al., 2011. Oil accumulation in the model green alga Chlamydomonas reinhardtii: characterization, variability between common laboratory strains and relationship with starch reserves. BMC Biotechnol. 11 7-7.
Starr, J.M., et al., 2014. Environmentally relevant mixing ratios in cumulative assessments: a study of the kinetics of pyrethroids and their ester cleavage metabolites in blood and brain; and the effect of a pyrethroid mixture on the motor activity of rats. Toxicology 320, 15–24.
Strašková, A., et al., 2019. Pigment-protein complexes are organized into stable microdomains in cyanobacterial thylakoids. Biochim. Biophys. Acta Bioenerg. https://doi.org/10.1016/j.bbabio.2019.07.008.
Sullivan, D.R., et al., 1985. Determination of serum triglycerides by an accurate enzymatic method not affected by free glycerol. Clin. Chem. 31, 1227–1228.
Tan, Q., et al., 2017. Stereoselective quantification of triticonazole in vegetables by supercritical fluid chromatography. Talanta 164, 362–367.
Urzica, E.I., et al., 2013. Remodeling of membrane lipids in iron-starved Chlamydomonas. J. Biol. Chem. 288, 30246–30258.
Wan, J., et al., 2014. Response of the cyanobacterium Microcystis flos-aquae to levofloxacin. Environ. Sci. Pollut. Res. Int. 21, 3858–3865.
Wang, H., Joseph, J.A., 1999. Quantifying cellular oxidative stress by dichlorofluorescein assay using microplate reader11Mention of a trade name, proprietary product, or specific equipment does not constitute a guarantee by the United States Department of Agriculture and does not imply its approval to the exclusion of other products that may be suitable. Free Radic. Biol. Med. 27, 612–616.
Wang, J., et al., 2011. Generation of reactive oxygen species in cyanobacteria and green algae induced by allelochemicals of submerged macrophytes. Chemosphere 85, 977–982.
Wang, X., et al., 2019. Enantioselective degradation of chiral fungicides triticonazole and prothioconazole in soils and their enantioselective accumulation in earthworms Eisenia fetida. Ecotoxicol. Environ. Saf. 183, 109491.
Wang, Z.T., et al., 2009. Algal lipid bodies: stress induction, purification, and biochemical characterization in wild-type and starchless Chlamydomonas reinhardtii. Eukaryot. Cell 8, 1856–1868.
Xi, J., et al., 2019. Acute toxicity of triflumizole to freshwater green algae Chlorella vulgaris. Pestic. Biochem. Physiol. 158, 135–142.
Xie, X., et al., 2011. Toxic effect of tetracycline exposure on growth, antioxidative and genetic indices of wheat (Triticum aestivum L.). Environ. Sci. Pollut. Control Ser. 18, 566–575.
Ye, J., et al., 2010. Enantioselectivity in environmental risk assessment of modern chiral pesticides. Environ. Pollut. 158, 2371–2383.
Ye, J., et al., 2015. Enantioselective environmental toxicology of chiral pesticides. Chem. Res. Toxicol. 28, 325–338.
Zhang, Q., et al., 2015. Enantioselective bioactivity, acute toxicity and dissipation in vegetables of the chiral triazole fungicide flutriafol. J. Hazard Mater. 284, 65–72.
Zhang, Q., et al., 2018a. Mechanistic insights into stereospecific bioactivity and dissipation of chiral fungicide triticonazole in agricultural management. J. Agric. Food Chem. 66, 7286–7293.
Zhang, W., et al., 2016. Enantioselective toxic effects of cyproconazole enantiomers against Chlorella pyrenoidosa. Chemosphere 159, 50–57.
Zhang, Z., et al., 2018b. Enantioselective degradation and transformation of the chiral fungicide prothioconazole and its chiral metabolite in soils. Sci. Total Environ. 634, 875–883.
Zhekisheva, M., et al., 2002. Accumulation of oleic acid in Haematococcus pluvialis (Chlorophyceae) under nitrogen starvation or high light is correlated with that of astaxanthin esters. J. Phycol. 38, 325–331.
Zhou, Q., et al., 2009. Enantioselectivity in the phytotoxicity of herbicide imazethapyr. J. Agric. Food Chem. 57, 1624–1631.
Zienkiewicz, K., et al., 2016. Stress-induced neutral lipid biosynthesis in microalgae — molecular, cellular and physiological insights. Biochim. Biophys. Acta Mol. Cell Biol. Lipids 1861, 1269–1281.